International Journal of Pharmaceutics 427 (2012) 410–416

Contents lists available at SciVerse ScienceDirect

International Journal of Pharmaceutics

journal homepage: www.elsevier.com/locate/ijpharm

Pharmaceutical Nanotechnology

Preparation, characterization and pharmacokinetic studies of tacrolimus-dimethyl-β-cyclodextrin inclusion complex-loaded albumin nanoparticles

Shanshan Gao[b], Jun Sun[b], Dongjun Fu[b], Hongli Zhao[a], Minbo Lan[a], Feng Gao[a,b,c,*]

[a] Shanghai Key Laboratory of Functional Materials Chemistry, East China University of Science and Technology, Shanghai 200237, PR China
[b] Department of Pharmaceutics, School of Pharmacy, East China University of Science and Technology, Shanghai 200237, PR China
[c] Shanghai Key Laboratory of New Drug Design, East China University of Science and Technology, Shanghai 200237, PR China

ARTICLE INFO

Article history:
Received 15 November 2011
Received in revised form
30 December 2011
Accepted 24 January 2012
Available online 2 February 2012

Keywords:
FK506/DM-β-CD inclusion complex
BSA nanoparticle
Sustained-release

ABSTRACT

The purpose of the study is to develop a new formulation for clinically used anti-cancer agent tacrolimus (FK506) to minimize the severe side effects. Toward this end, a new formulation method has been developed by complexation of FK506 with an hydrophilic cyclodextrin derivative, heptakis (2,6-di-*O*-methyl)-β-cyclodextrin (DM-β-CD) using ultrasonic means. The resulting complex displays dramatically enhanced solubility of FK506. Then bovine serum albumin (BSA) nanoparticles were prepared directly from the preformed FK506/DM-β-CD inclusion complex by the desolvation-chemical crosslinking method, with the size of 148.4–262.9 nm. Stable colloidal dispersions of the nanoparticles were formed with zeta potentials of the range of −24.9 to −38.4 mV. The entrapment efficiency of FK506 was increased as high as 1.57-fold. Moreover, notably FK506 was released from the nanoparticles in a sustained manner. As demonstrated, pharmacokinetic studies reveal that, as compared with FK506-loaded BSA nanoparticles, the FK506/DM-β-CD inclusion complex-loaded BSA nanoparticles have significant increase at T_{max}, $t_{1/2}$, *MRT* and decrease at C_{max}. In summary, these results suggest that the drug/DM-β-CD inclusion complex-loaded BSA nanoparticles display significantly improved delivery efficiency for poorly soluble FK506 or its derivatives.

1. Introduction

Tacrolimus (FK506, molecular weight of 822.05, water solubility of 1.3 μg/ml), a hydrophobic macrolide lactones natural product isolated from by *Streptomyces tsukubaensis*, exerts potent immunosuppressive effects and has been in clinical use as prophylaxis against organ rejection after liver and renal transplantation (Hidetoshi et al., 2001). Recently, it has been reported that FK506 can be widely distributed in the body with a high degree binding of red blood cells and plasma proteins. However, the distribution is significantly affected by individual differences, and the administration routes. For example, the gastrointestinal tract has a narrow therapeutic window due to low bioavailability (Taher et al., 2009), and side effects. In addition, FK506 is known to exhibit low oral bioavailability and a wide range of variability in absorption, ranging from 4 to 89% in kidney and liver transplant recipients (Venkataramanan et al., 1995). For the intravenous administration, because of its low solubility, some solubilizer or injection oil was used, thus inducing greater toxicity.

β-Cyclodextrin (β-CD) and its derivatives, as distinct solubilizers, have received considerable attention, giving prominence to their low biotoxicity and high biocompatibility. As attractive materials for drug inclusion, β-CD can be further chemically modified to improve its physicochemical properties (Hassan and Asghar, 2009; Song et al., 2009). A number of studies have shown that adding β-CD can improve the loading efficiency of nanoparticles and slow down the release of drugs (Alexander and Maria, 2007; Boudad et al., 2001; Maestrelli et al., 2006). Ferreira and collaborators prepared inclusion complexes with hydroxypropyl-β-cyclodextrin and the aqueous solubility of the drug increased linearly with the concentration of the cyclodextrins (Denise et al., 2004). The cavity depth and surface activity of 2,6-di-*O*-methyl-β-cyclodextrin (DM-β-CD), a derivative of β-CD, improved significantly, as well as the solubility increased as much as by 25 times (Gamal et al., 1986). Various β-CD derivatives have been evaluated to probe their enhancing effect on solubility and stability of FK506 in rats. It was found that DM-β-CD had a dramatic improvement on solubilization and stabilization of FK506 (Hidetoshi et al., 2001).

Modern nanotechnology is considered as an emerging and converging technology (Roco, 2008) and that is said to be one of the

* Corresponding author at: Department of Pharmaceutics, School of Pharmacy, East China University of Science and Technology, 130 Meilong Road, Shanghai 200237, PR China. Tel.: +86 21 6425 2449; fax: +86 21 6425 8277.
E-mail address: fgao@ecust.edu.cn (F. Gao).

0378-5173/$ – see front matter © 2012 Elsevier B.V. All rights reserved.
doi:10.1016/j.ijpharm.2012.01.054

key technologies of the 21st century. Nanotechnology is widely seen as having huge potential to bring benefits to many areas of research and application. Studies have shown that albumin nanoparticle has a higher capacity of loading hydrophilic drugs, better performance of controlled release and more stability of storage (MacAdam et al., 1997; Orapin et al., 1993). Furthermore, albumin offers several notable characteristics, including safety, non-toxic, non-immunogenicity, biodegradability and good biocompatibility. Therefore it serves an attractive drug delivery system. After release of drugs, albumin nanoparticles can be absorbed by body through the metabolic decomposition without producing harmful residual substances (Langer et al., 2003; Yun et al., 2007). In addition, the albumin molecule has many functional groups, thus allowing for convenient functionalizations for various purposes. General methods for preparation of albumin nanoparticles include ultrasonic emulsification, desolvation method, pH coagulation, salting, etc. (Langer et al., 2003; Muller et al., 1996; Merodio et al., 2001; Weber et al., 2000). For the desolvation method, several factors can affect albumin nanoparticles such as drugs, the dosage of albumin and the preparation of albumin nanoparticles including dehydrolyzing agent, cross linking agent, pH, cross linking time and stirring speed (Guilin et al., 2008; Hyuncheol et al., 2009; Vogel et al., 2002). With the carrier of albumin, albumin nanoparticles are solid sphere obtained by curing and separation, which can encapsulate and adsorb different kinds of drugs such as polypeptides, vaccines and gene to be used in varied disease. Controlled the nanosize of albumin nanoparticles can not only reduce toxicity but achieve certain sustained effect when used in intravenous. Currently, the research of FK506-loaded nanoparticles has mainly focused on the use of polylactic acid and acrylic acid as the carrier material (Nakaoka et al., 1995; Nakase et al., 2000). The study on the FK506/DM-β-CD inclusion complex-loaded albumin nanoparticles has not been reported.

The purpose of the present study is to develop a novel nano-drug delivery system (NDDS), drug/DM-β-CD inclusion complex-loaded BSA nanoparticles. Firstly, FK506 was complexed to a hydrophilic cyclodextrin derivative via the formation of inclusion complex of the drug with DM-β-CD by an ultrasonic method. Then, FK506/DM-β-CD inclusion complex-loaded bovine serum albumin (BSA) nanoparticles were prepared by desolvation-chemical crosslinking method. The physicochemical characteristics were determined (i.e. entrapment efficiency, loading efficiency, in vitro release, size distribution of the developed nanoparticles). In addition, pharmacokinetic parameters of these nanoparticles were investigated in rats.

2. Materials and methods

2.1. Chemicals and reagents

FK506 (purity > 99.1%) was purchased from Qiao Chemical Co. Ltd. (Shanghai, China). DM-β-CD (purity > 99.0%) was purchased from Kaiyang Biotech Co. Ltd. (Shanghai, China). Bovine serum albumin (BSA, purity 96–99%) was purchased from Yuanju Bio-tech Co. Ltd. (Shanghai, China). Glutaraldehyde was obtained from Chinese Medicine Group Shanghai Chemical Reagent Company (Shanghai, China). Male Wistar rats used in the experiments were supplied by the Department of Laboratory Animal Science, Fudan University, treated according to the protocols evaluated and approved by the Ethical Committee of the University. All other reagents used in this study were high performance liquid chromatography (HPLC) or reagent grade.

2.2. Determination of FK506 by HPLC in vitro and in vivo

FK506 was determined using a modified reverse-phase HPLC system (Lee et al., 1995). This system consisted of two model LC-10ADvp pumps, an SPD-10AVP diode-array UV–Vis detector and an SCL-10AVP system controller. Chromatographic separation was achieved on a Platisil ODS-C_{18} column (4.6 mm × 250 mm, 5 μm, Dikma, Beijing, China). The mobile phase was consisted of acetonitrile–water (60:40, v/v) and adjusted to pH 2.7 with phosphoric acid, which delivered at an isocratic flow rate of 1.0 ml/min at the room temperature. The detection wavelength was set at optical density of 215 nm. The injection volume was 20 μl and the retention time was 9.8 min. Standard curve produced by the FK506 assay method appeared in a good linear correlation in the solution concentration range. The usefulness of the assay was confirmed by the analysis of plasma samples in rats.

2.3. Preparation of empty BSA nanoparticles

Empty BSA nanoparticles were prepared using a previously described desolvation technique (Muller et al., 1996). In principle, BSA was dissolved at concentrations of 10, 25, 50, 75.100 and 150 mg/ml in 2 ml of 10 mM sodium chloride and the pH of the solution was adjusted titrated to 2, 3, 4, 5, 6, 7, 8, 9, 10, 11 and 12, respectively. The resulting solutions were filtered through a 0.22-μm filter membrane. Aliquots (2 ml) of the BSA solution were transformed into nanoparticles by the continuous addition of 4–8 ml ethanol under constant stirring (600 rpm) at room temperature. The ethanol addition was performed using a constant flow pump which enabled nanoparticle preparation at a define rate of 1.0 ml/min. Following the desolvation process the particles were stabilized by the addition of an aqueous (150 μl) 4.17% glutaraldehyde solution. The crosslinking process was performed under stirring of the suspension over a time period of 18 h at room temperature. The resulting nanoparticles were purified repeated centrifugation at 12,000 rpm for 20 min, and redispersed in water by ultrasonication in order to eliminate excipients such as ethanol and glutaraldehyde. Dry nanoparticles were obtained after freeze drying with 3% mannitol as lyophilized protection agent.

2.4. Degradation of BSA nanoparticles

Nanoparticle degradation was determined in the absence and presence of trypsin. BSA nanoparticles were prepared as outline above except for the extent of particle stabilization. A known amount of the freeze-dried BSA nanoparticles was placed in phosphate buffer solution (PBS, pH 6.8) with and without 1% trypsin and incubated at 37 °C water-bath. The turbidity of the nanoparticle suspensions was measured photometrically at a wavelength of 565 nm by UV spectrophotometer (T6-1650F, Beijing, China). The BSA nanoparticle preparation was performed in three independent samples. The analytical results were given as mean value and standard deviation of these samples.

$$\text{degradation rate}\,(\%) = \frac{\text{initial concentration of the nanoparticles} - t\ \text{time concentration of the nanoparticles}}{\text{initial concentration of the nanoparticles}} \times 100 \quad (1)$$

2.5. Swelling of BSA nanoparticles

The swelling degrees of the BSA nanoparticles in demineralized water were determined in 24 h. A known amount of BSA nanoparticles was dispersed in water and the shaking rate was 150 rpm. After incubation at 37 °C at specified time, the suspension was

centrifuged at 12,000 rpm for 20 min and the precipitate was weighted. The swelling degree was calculated according to Eq. (2):

$$\text{swelling degree}(\%) = \frac{\text{wet weight of nanoparticles} - \text{dry weight of nanoparticles}}{\text{dry weight of nanoparticles}} \times 100 \quad (2)$$

2.6. Preparation of FK506/DM-β-CD inclusion complex

The solid FK506/DM-β-CD inclusion complexes in a ratio of 1:3, 1:5 or 1:10 were prepared by ultrasonic method (Hirayama et al., 1996). The calculated amounts of FK506 and DM-β-CD were weighed and dissolved in 50% or 75% ethanol, which was under ultrasound thoroughly for 15 or 30 min at specified temperature. After evaporation of the solvent, the solid FK506/DM-β-CD inclusion complexes were washed twice, then dried under reduced pressure at room temperature and stored in a desiccator.

2.7. Preparation of FK506-loaded BSA nanoparticles

The FK506-loaded BSA nanoparticles were prepared using the desolvation method. FK506 (0, 2, 2.5, 3, 3.5, 4 and 5 mg/ml) in ethanol (1 ml) was added into 2 ml of BSA solution (50 mg/ml) at room temperature. BSA nanoparticles were transformed by the continuous addition of 3 ml ethanol under stirring (800 rpm) at room temperature. The next steps were performed as described in Section 2.2.

2.8. Preparation of FK506/DM-β-CD inclusion complex-loaded BSA nanoparticles

For the formation of the FK506/DM-β-CD inclusion complex-loaded BSA nanoparticles, a known amount of FK506/DM-β-CD inclusion complexes (18, 21, 24, 30, 45 and 60 mg) was dissolved in 2 ml BSA solution and ethanol (4 ml) was added with a tubing pump at the rate of 1 ml/min under constant stirring (600 rpm) at room temperature. The next steps were performed as described in Section 2.2.

2.9. Physicochemical characterization of BSA nanoparticles

Mean diameter, size distribution and zeta potential of the prepared nanoparticles were determined by dynamic light scattering using a DB-525 laser particle size instrument (Brookhaven Instruments Corp., USA).

Morphological examination of the freeze-dried nanoparticles was conducted by scanning electron microscopy (SEM). Nanoparticles were freeze-dried, coated with platinum and observed with a scanning electron microscope (JSM-6360LV, JEOL Ltd., Tokyo, Japan).

2.10. Yield of BSA nanoparticles

After preparation of nanoparticles, the supernatant of nanoparticle solution was isolated by centrifugation for 20 min (4 °C, 12,000 rpm). The supernatant diluted by demineralized water was incubated with coomassie brilliant blue for 10 min. BSA was assayed by ultraviolet spectrophotometer (General Analysis of General Instrument, Beijing, China) at 595 nm (Bradford, 1976). Standard curvilinear equation was substituted to calculate the concentration of BSA out of desolvated.

$$\textit{yield}(\%) = \frac{\text{amount of BSA in nanoparticles}}{\text{total amount of BSA}} \times 100 \quad (3)$$

2.11. Entrapment efficiency and loading efficiency

After preparing nanoparticles, we collected the supernatant and added ethanol into it to precipitate protein. The concentration of FK506 in supernatant was determined by HPLC. Entrapment efficiency (EE) and loading efficiency (LE) were calculated as follows.

$$\text{entrapment efficiency}(\%) = \frac{\text{amount of FK506 in nanoparticles}}{\text{total amount of FK506}} \times 100 \quad (4)$$

$$\text{loading efficiency}(\%) = \frac{\text{amount of FK506 in nanopaticles}}{\text{total amount of nanoparticles}} \times 100 \quad (5)$$

2.12. In vitro drug release of nanoparticles

An incubation method was used for investigation of drug release from the FK506/DM-β-CD inclusion complex-loaded BSA nanoparticles. The nanoparticles (10 mg) were suspended in 50 ml of PBS containing 0.1% (v/v) Tween-80 (pH 7.4), and then immersed in a constant temperature water bath (37.0 ± 0.5 °C) with a shaking rate of 100 rpm. At various time intervals, sample (1 ml) were withdraw and replaced by an equal volume of fresh PBS, then sample was filtered through a 0.22-μm filter unit and assayed by HPLC. The accumulative release percentage was calculated at each time point.

2.13. Animal testing

Male Wistar rats (250 ± 15 g), fasting overnight, were intravenously given a dose of equivalent to FK506 0.5 mg/kg. An ethanol solution of FK506 was diluted with saline immediately before injection. Nine rats were randomly divided into three groups, Group A: FK506 treated group; Group B: FK506-loaded BSA nanoparticles treated group; Group C: the FK506/DM-β-CD inclusion complex-loaded BSA nanoparticles treated group. The blood samples (0.2 ml) were drawn from the rat's tail vein at a designated time intervals. Blood samples were centrifuged to obtain plasma (100 μl). Ether (2 ml) was added into the plasma and mixed for 2 min. The mixture was centrifuged at 10,000 rpm for 2 min and the upper (1.5 ml) was transferred and dried by nitrogen gas. The residue was dissolved with 200 μl mobile phase and the FK506 concentration in plasma was assayed by HPLC.

2.14. Statistical analysis

Multiple group comparison was conducted by one-way analysis of variance (ANOVA) and then by LSD using statistical software (SPSS, Chicago). All data are presented as a mean value with its standard deviation indicated (mean ± SD). p-Values less than 0.05 were considered to be statistically significant.

3. Result and discussion

3.1. Preparation and characterization of empty BSA nanoparticles

In this study, we investigated the effects of the pH, the concentration of BSA and the dosage of ethanol on the yield and mean particle size in the preparation of empty BSA nanoparticles

Table 1
Characterization of BSA nanoparticles by desolvation-chemical crosslinking method (mean ± SD, $n = 3$).

pH	BSA (mg/ml)	Ethanol (ml)	Morphology	Yield (%)	Particle size (nm)	PI
2	50	8	Unformed	–	–	–
3	50	8	Unformed	–	–	–
4	50	4	Spherical	<30	–	–
5	50	4	Aggregated	–	–	–
6	50	4	Aggregated	–	–	–
7	50	4	Spherical	96.3 ± 0.06	284.6 ± 14.9	0.12
8	10	4	Aggregated	–	–	–
8	25	4	Spherical	99.9 ± 0.06	191.9 ± 4.2	0.24
8	50	4	Spherical	97.0 ± 0.10	151.4 ± 9.0	0.28
8	75	4	Spherical	96.2 ± 0.06	284.6 ± 1.9	0.18
8	100	4	Spherical	95.2 ± 0.15	296.9 ± 11.0	0.03
8	150	4	Aggregated	–	–	–
8	50	5	Spherical	99.0 ± 0.06	217.0 ± 11.1	0.11
8	50	6	Spherical	99.5 ± 0.10	221.3 ± 3.2	0.19
8	50	8	Spherical	99.8 ± 0.12	270.5 ± 15.8	0.23
9	50	4	Spherical	97.5 ± 0.06	148.4 ± 7.9	0.31
10	50	4	Spherical	96.4 ± 0.10	170.4 ± 5.3	0.28
11	50	4	Spherical	<30	–	–
12	50	4	Unformed	–	–	–

PI: polydispersity index; –: unmeasured.

(Table 1). When the value of pH was more than 12 or less than 3, BSA nanoparticles failed to form because of the excessive electric charge. At pH 4 or pH 11, BSA nanoparticles were obtained with a low yield (<30%). BSA nanoparticles aggregated at pH 5 or pH 6 because the value of pH was close to the isoelectric point (pH 5.4) of BSA, which maybe cause a sharp decline in the solubility of BSA, resulting in a lot of precipitation and aggregation. However, the BSA nanoparticles were obtained with ideal diameter at pH 7–9. When the concentration of BSA was more than 150 mg/ml, even a small amount of additional ethanol was easy to cause aggregation. When the concentration of BSA was less than 10 mg/ml, an addition of 4-ml ethanol was excessive for it, which resulted in the aggregation of BSA. The more consumption of ethanol was, the higher degree of desolvation BSA had, leading to the high yield of nanoparticles, but the diameter of BSA nanoparticles increased slightly. Base on these studies, we obtained desired BSA nanoparticles at pH of 8–9 with 148.4–151.4 nm of average diameter and 97.5 ± 0.1% of yield, spherical and fine distributed when the concentration of BSA was 50 mg/ml and the consumption of ethanol was 4 ml.

3.2. Degradation and swelling of BSA nanoparticles

Degradation of BSA nanoparticles was investigated in the absence and presence of an enzyme. In the absence of 1% trypsin, it took 24 h for less than 3% degradation of BSA nanoparticles while 18.8% degradation was achieved in the presence of trypsin (Fig. 1). Albumin nanoparticles were known to swell in an aqueous environment due to hydration. Following hydration, pores, cavities, and/or channels were formed in the particle matrix. The swelling degree of BSA nanoparticles reached 83.0% in 0.5 h and decreased to 40.4% in 2 h (Fig. 2). After the process of dynamic balance, the swelling degree was stabilized at 45.4%. The study indicated that in the initial stage, nanoparticles swelled rapidly by taking-up through port hole resulting in the quick release of the drug in the surface or the superficial of nanoparticles. After reaching equilibrium, the drug released slowly through the frame or the degradation of nanoparticles. In the present study, we supposed the carrier had a little sustained release effect.

3.3. Preparation and characterization of FK506/DM-β-CD inclusion complex

The inclusion complex was prepared by an ultrasonic method. It was found that the influence of weight ratio (FK506/DM-β-CD) on

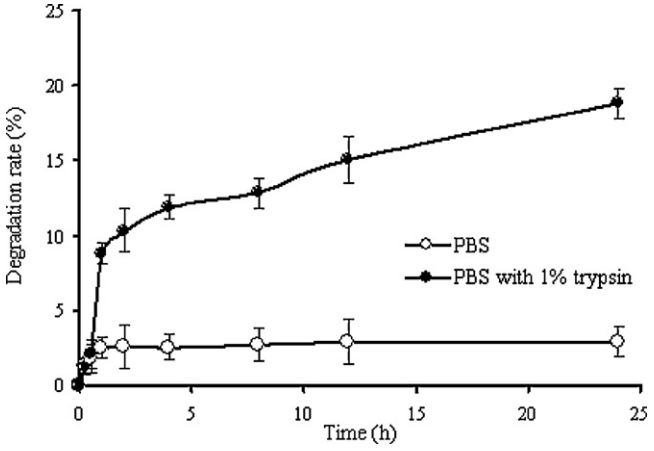

Fig. 1. The degradation process of BSA nanoparticles in PBS. The BSA nanoparticles were in the absence or presence of 1% trypsin in PBS (pH 6.8). The diameter of BSA nanoparticles was 148.4 ± 7.9 nm as shown in Table 1. Data were presented as mean ± SD ($n = 3$).

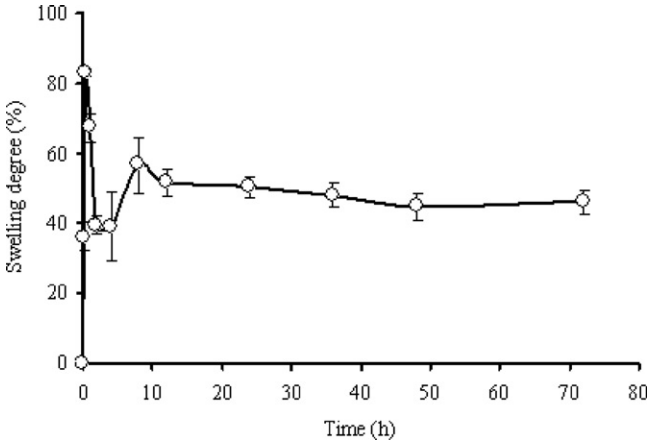

Fig. 2. The swelling degree of BSA nanoparticles in water. The BSA nanoparticles were in water. The diameter of BSA nanoparticles was 148.4 ± 7.9 nm as shown in Table 1. Data were presented as mean ± SD ($n = 3$).

Table 2
Characterization of FK506/DM-β-CD inclusion complex prepared by ultrasonic method (mean ± SD, $n = 3$).

FK506: DM-β-CD (w/w)	Temperature (°C)	Time (min)	Ethanol (%)	EE (%)	LE (%)	Yield (%)
1: 3	20	15	75	16.7 ± 2.9	5.6 ± 0.7	71.0 ± 2.3
1: 5	20	15	50	20.4 ± 2.2	4.9 ± 0.5	72.5 ± 1.9
	20	30	75	38.9 ± 2.3	8.8 ± 0.5	74.4 ± 1.6
	40	15	75	25.0 ± 2.4	6.2 ± 0.6	76.3 ± 2.3
	40	30	50	53.0 ± 2.9	12.0 ± 0.7	73.0 ± 1.5
	40	30	75	57.3 ± 2.7	12.4 ± 0.3	76.8 ± 2.1
1: 10	20	15	75	71.0 ± 4.7	7.0 ± 0.3	82.7 ± 2.7

EE, entrapment efficiency; LE, loading efficiency.

the entrapment efficiency and loading efficiency was more significant than that of the ethanol concentration (Table 2). However, in line with the process of ultrasonic, precipitation emerged in the bottom of the tube after several days using 50% ethanol as solvent. It indicated that some FK506 released from the FK506/DM-β-CD inclusion complexes and precipitated because of its limited solubility in 50% ethanol. Therefore, 75% ethanol was adopted. On the other hand, higher temperature and longer reaction time resulted in better entrapment efficiency and loading efficiency, indicative of increasing temperature or extending ultrasonic time could increase the contact opportunity between FK506 molecule and DM-β-CD molecule to make inclusion complexes forming more easily. According to the single factor test, the optimal formation condition was kept a ratio of DM-β-CD: FK506 as 5:1 (w/w) and 75% ethanol under ultrasound for 30 min at 40 °C. The entrapment efficiency, loading efficiency and yield of FK506/DM-β-CD inclusion complex were 57.3 ± 2.7%, 12.4 ± 0.3%, and 76.8 ± 2.1%, respectively. With the addition of DM-β-CD, the solubility of FK506 increased more than 200-fold. It implied that the cavity of DM-β-CD fit the FK506 molecule comfortably (Hidetoshi et al., 2001). The further study for the impact of increase of temperature or extension of ultrasonic time on the stability of FK506 was still required.

3.4. Preparation and characterization of FK506/DM-β-CD inclusion complex-loaded BSA nanoparticles

In this study, based on the empty BSA nanoparticles (Fig. 3A), we obtained the FK506 loaded-BSA nanoparticles and FK506/DM-β-CD inclusion complex-loaded BSA nanoparticles with near-spherical shape (Fig. 3B and C). The influence of concentration of FK506 on the characterization of BSA nanoparticles was investigated (Table 3). The diameter of nanoparticles increased from 148.4 to 262.9 nm while the concentration of FK506 changed from 0 to 10 mg/ml, which might be related to the encapsulation of more FK506 or FK506/DM-β-CD inclusion complex. The diameter of nanoparticles was between 100 and 270 nm, which was beneficial for BSA nanoparticles entering into the systemic circulation (Langer et al., 2003). On the other hand, when the concentration of FK506 increased, though the loading efficiency increase slightly, more drug assembled in the surface of nanoparticles, which led to the zeta potential change from −38.4 mV to −24.9 mV. With the same concentration of FK506, the entrapment efficiency of FK506/DM-β-CD inclusion complex-loaded BSA nanoparticles was 1.57-fold larger than that of FK506-loaded BSA nanoparticles. It may be because that hydrophilic BSA had poor capability to encapsulate hydrophobic FK506. On the contrary, insoluble FK506 was suitable for the hydrophobic cavity of DM-β-CD whose hydrophilic outer surface could be wrapped into BSA nanoparticles easily, which therefore improved the solubility of FK506 and enabled more FK506 encapsulated in BSA/DM-β-CD nanoparticles. On the whole, taking into account the size, the zeta potential, especially the entrapment efficiency, we used FK506/DM-β-CD inclusion complex-loaded BSA nanoparticles with 3.5 mg/ml of FK506 for the later study which the entrapment efficiency of that reached the maximum 95.5 ± 0.5%.

3.5. In vitro drug release of nanoparticles

The accumulative release of FK506/DM-β-CD inclusion complex-loaded BSA nanoparticles was 10.8 ± 0.8% at 0.5 h, 20.7 ± 1.7% at 24 h, and 39.7 ± 4.3% at 48 h, respectively (Fig. 4). Meanwhile, the accumulative release of FK506-loaded BSA nanoparticles was 22.3 ± 0.9% at 0.5 h, 34.9 ± 1.7% at 24 h and 45.6 ± 3.2% at 48 h, respectively. Compared with FK506-loaded BSA nanoparticles, the FK506/DM-β-CD inclusion complex-loaded BSA nanoparticles had smaller burst release by 0.5-fold, showing the sustained-release effect. From the in vitro release profiles, it seemed that some drug was not been incorporated but presented on the surface of nanoparticles. The plausible reason was that the process of FK506 released into the medium from the FK506/DM-β-CD inclusion complex-loaded BSA nanoparticles fit a biphasic release process. Briefly, FK506 released from the surface of nanoparticles the initial stage, and then released from the FK506/DM-β-CD inclusion complex and BSA nanoparticles. The surface presence of the drug was also in agreement with the result of zeta potential.

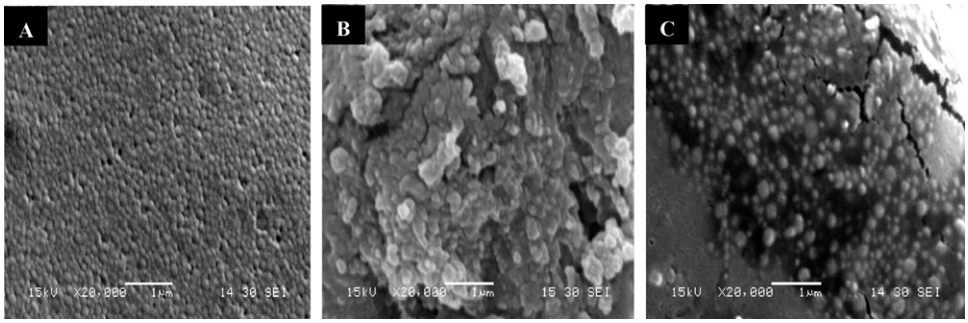

Fig. 3. The SEM photographs of BSA nanoparticles. (A) Empty BSA nanoparticles, (B) FK506-loaded BSA nanoparticles, (C) FK506/DM-β-CD inclusion complex-loaded BSA nanoparticles.

Table 3
Characterization of FK506/DM-β-CD-loaded BSA nanoparticles by desolvation-chemical crosslinking method (mean ± SD, $n = 3$).

FK506 (mg/ml)	FK506/DM-β-CD (w/w)	EE (%)	LE (%)	Particle size (nm)	PI	Zeta potential (mV)	Yield (%)
0	0/0	–	–	148.4 ± 7.9	0.21	−37.8 ± 0.3	97.5 ± 0.1
	0/18	–	–	225.1 ± 10.3	0.24	−38.0 ± 0.3	95.9 ± 0.4
2	2/0	43.9 ± 1.7	0.88 ± 0.04	183.2 ± 2.1	0.27	−27.5 ± 0.5	98.1 ± 0.2
2.5	2.5/0	40.7 ± 0.4	1.02 ± 0.01	217.3 ± 4.1	0.21	−28.1 ± 0.6	97.7 ± 0.2
3	3/0	41.6 ± 1.4	1.25 ± 0.04	219.0 ± 9.2	0.25	−27.7 ± 0.2	97.6 ± 0.1
	1/5	83.4 ± 1.1	2.12 ± 0.07	225.8 ± 1.1	0.13	−33.3 ± 0.2	94.7 ± 0.3
3.5	3.5/0	60.6 ± 2.5	2.12 ± 0.09	218.5 ± 6.0	0.26	−26.4 ± 0.4	97.6 ± 0.2
	1/5	95.5 ± 0.5	3.20 ± 0.04	245.2 ± 7.5	0.15	−38.4 ± 0.5	95.6 ± 0.3
4	4/0	31.5 ± 0.4	1.74 ± 0.12	220.1 ± 3.4	0.15	−33.1 ± 0.3	93.8 ± 0.4
	1/5	37.2 ± 4.2	1.49 ± 0.17	224.5 ± 6.1	0.21	−35.5 ± 0.8	97.5 ± 0.1
5	5/0	29.5 ± 3.0	1.47 ± 0.15	233.5 ± 5.3	0.18	−30.2 ± 0.3	96.5 ± 0.2
	1/5	67.6 ± 1.6	4.13 ± 0.08	241.1 ± 5.0	0.12	−31.9 ± 0.5	93.3 ± 0.4
7.5	1/5	55.8 ± 1.7	4.19 ± 0.12	252.1 ± 1.7	0.16	−32.9 ± 0.6	93.5 ± 0.7
10	1/5	42.3 ± 1.1	4.23 ± 0.11	262.9 ± 15.1	0.25	−24.9 ± 0.9	95.1 ± 0.6

EE, entrapment efficiency; LE, loading efficiency; PI, polydispersity index; –, unmeasured.

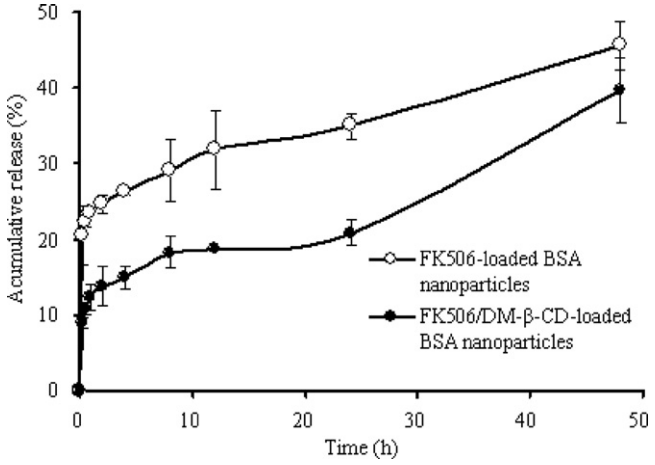

Fig. 4. Accumulative drug release of BSA nanoparticles. Accumulative release of FK506-loaded BSA nanoparticles and FK506/DM-β-CD inclusion complex-loaded BSA nanoparticles. The release medium was in PBS (pH 7.4) containing 0.1% Tween-80. Data were expressed as mean ± SD ($n = 3$).

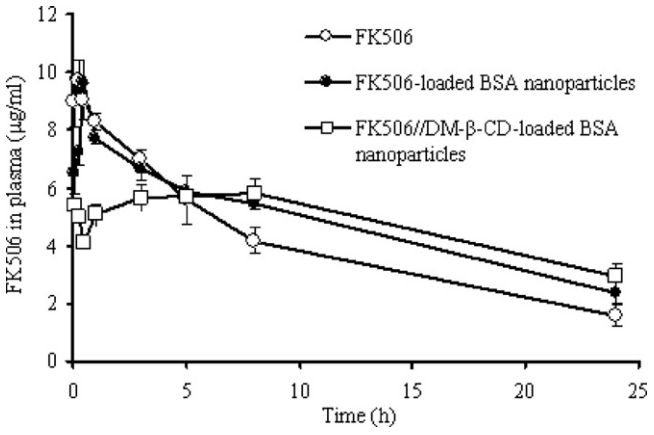

Fig. 5. Plasma concentration–time curve of FK506 after a single intravenous administration in rats. Rats were followed a single dose of intravenous FK506 (5 mg/kg). Data were expressed as mean ± SD ($n = 3$).

3.6. Animal testing

The plasma concentrations of FK506 in rats were quantified by the assay up to 24 h (Fig. 5). After intravenous administrated the same dose of FK506, the plasma concentration of FK506 reached its C_{max} at 480 min for the FK506/DM-β-CD inclusion complex-loaded BSA nanoparticles while it was at 15 min for FK506, and 30 min for FK506-loaded BSA nanoparticles, respectively (Table 4). The reason was probably due to a second-order release process which implied that FK506 required a longer time to reach peak after released from FK506/DM-β-CD inclusion complex. As observed, until 24 h after a single administration, the FK506 plasma concentration of the FK506/DM-β-CD inclusion complex-loaded BSA nanoparticles was higher than that of FK506 or FK506-loaded BSA nanoparticles. These in vivo results were consistent with previously obtained accumulative release curves in vitro, indicating that the FK506/DM-β-CD inclusion complex-loaded BSA nanoparticles had a delayed-release effect. Compared with FK506 or FK506-loaded BSA nanoparticles, the FK506/DM-β-CD inclusion complex-loaded BSA nanoparticles had no apparent differences in $AUC_{0-24\,h}$. However, in comparison with FK506-loaded BSA nanoparticles, the FK506/DM-β-CD inclusion complex-loaded BSA nanoparticles had significant increase at T_{max}, $t_{1/2}$, MRT and decrease at C_{max}, respectively. Specifically, although the $AUC_{0-24\,h}$ of the FK506/DM-β-CD inclusion complex-loaded BSA nanoparticles was close to FK506-loaded BSA nanoparticles, they obtained a much longer MRT, which stood for prolonged drug duration in vivo. Pharmacokinetic results showed that FK506/DM-β-CD inclusion complex-loaded BSA nanoparticles also could make FK506 release more stably and continuously.

Table 4
Pharmacokinetic parameters of FK506/DM-β-CD-loaded BSA nanoparticles in rats following a single dose of intravenous administration (0.5 mg/kg) (mean ± SD, $n = 3$).

Treatment	C_{max} (μg/ml)	T_{max} (min)	$t_{1/2}$ (min)	$AUC_{0-24\,h}$ (μg min/ml)	MRT (h)
FK506	9.69 ± 0.84	15 ± 0	445 ± 163	5816 ± 546	7.65 ± 0.44
FK506-loaded BSA nanoparticles	9.64 ± 0.44	30 ± 0	678 ± 123	6824 ± 154	8.67 ± 0.47
FK506/DM-β-CD-loaded BSA nanoparticles	6.13 ± 1.87*	480 ± 151**	1407 ± 81**	6842 ± 206	9.72 ± 0.31*

C_{max}, maximum plasma concentration following drug administration; T_{max}, time to reach maximum blood concentration following drug administration; $t_{1/2}$, half-time; $AUC_{0-24\,h}$, the area under the concentration–time curve; MRT, mean residence time.
The FK506/DM-β-CD-loaded BSA nanoparticles had significant difference at C_{max}, T_{max}, $t_{1/2}$ and MRT as compared with FK506-loaded BSA nanoparticles.
* $p < 0.05$, by ANOVA.
** $p < 0.01$ by ANOVA.

4. Conclusion

In the study, the FK506/DM-β-CD inclusion complex-loaded BSA nanoparticles have been successfully prepared by the desolvation-chemical crosslinking method. The work represented the first example using a drug delivery system of albumin/DM-β-CD as a carrier for delivery of poorly soluble FK506. The drug delivery system with uniform particle size, posses higher entrapment efficiency and lower burst-release rate. The study in vitro and in vivo also indicated this drug delivery system had sustained-release effect which enabled FK506 release more stably and continuously. These features render it as general delivery system, which could be used for poorly soluble FK506 or its derivatives.

Acknowledgements

The authors acknowledge the financial support from Shanghai nanotechnology leading academic discipline foundation (No. 0852nm05900) and 111 program of China (No. B07023). This work was supported by Science and Technology Commission of Shanghai Municipality (STCSM, contract Nos. 10dz2220500 and 11dz2260600).

References

Alexander, H.K., Maria, J.A., 2007. Chitosan/cyclodextrin nanoparticles as macromolecular drug delivery system. Int. J. Pharm. 34, 134–142.

Boudad, H., Legrand, P., Lebas, G., 2001. Combined hydroxypropyl-β-cyclodextrin and poly(alkylcyanoacrylate) nanoparticles intended for oral administration of saquinavir. Int. J. Pharm. 218, 113–124.

Bradford, M.M., 1976. A rapid and sensitive method for quantitation of microgram quantities of protein utilizing the principle of protein-dye binding. Anal. Biochem. 72, 248–254.

Denise, A.F., Antonio, G.F., Lucinéia, V., Alberto, F.N., Anselmo, G.O., 2004. Analysis of the molecular association of rifampicin with hydroxypropyl-β-cyclodextrin. Braz. J. Pharm. Sci. 40, 43–51.

Gamal, A.E., Terada, K., Yamamoto, K., Nakai, Y., 1986. Molecular behavior, dissolution characteristics and chemical stability of aspirin in the ground mixture and in the inclusion complex with di-O-methyl-β-cyclodextrin. Int. J. Pharm. 31, 25–31.

Guilin, W., Kevin, S., Sufeng, Z., 2008. Preparation of BMP-2 containing bovine serum albumin (BSA) nanoparticles stabilized by polymer coating. Pharm. Res. 25, 2896–2909.

Hassan, N., Asghar, K., 2009. Investigation diffusion mechanism of β-lactam conjugated telechelic polymers of PEG and β-cyclodextrin as the new nanosized drug carrier devices. Carbohyd. Polym. 76, 46–50.

Hidetoshi, A., Kiyokazu, Y., Kouzou, M., 2001. Comparative studies of the enhancing effects of cyclodextrins on the solubility and oral bioavailability of tacrolimus in rats. J. Pharm. Sci. 90, 690–701.

Hirayama, F., Minami, K., Uekama, K., 1996. In vitro evaluation of biphenylyl acetic acid-β-cyclodextrin conjugates as colon-targeting prodrugs: drug release behavior in rat biological media. J. Pharm. Pharmacol. 48, 27–31.

Hyuncheol, K., Shaun, B.R., Karl, G.C., 2009. Investigating the movement of intravitreal human serum albumin nanoparticles in the vitreous and retina. Pharm. Res. 26, 329–337.

Langer, K., Balthasar, S., Vogel, V., Dinauer, N., von Briesen, H., Schubert, D., 2003. Optimization of the preparation process for human serum albumin (HSA) nanoparticles. Int. J. Pharm. 257, 169–180.

Lee, M.J., Robert, M.S., William, J.J., 1995. Physicochemical, pharmacokinetic and pharmacodynamic evaluation of liposomal tacrolimus (FK 506) in rats. Pharm. Res. 12, 1055–1059.

MacAdam, A.B., Shafi, Z.B., James, S.L., Marriott, C., Martin, G.P., 1997. Preparation of hydrophobic and hydrophilic albumin microspheres and determination of surface carboxylic acid and amino residues. Int. J. Pharm. 151, 47–55.

Maestrelli, F., Garcia-Fuentes, M., Mura, P., Alonso, M.J., 2006. A new drug nanocarrier consisting of chitosan and hydoxypropylcyclodextrin. Eur. J. Pharm. Biopharm. 63, 79–86.

Muller, B.G., Leuenberger, H., Kissel, T., 1996. Albumin nanospheres as carrier for passive drug targeting: an optimized manufacturing technique. Pharm. Res. 13, 32–37.

Merodio, M., Irache, J.M., Eclancher, F., 2001. Ganciclovir-loaded albumin nanoparticles: characterization and in vitro release properties. Eur. J. Pharm. Biopharm. 12, 249–253.

Nakase, H., Okazaki, K., Tabata, Y., Uose, S., Ohana, M., Uchida, K., Matsushima, Y., Kawanami, C., Oshima, C., Ikada, Y., Chiba, T., 2000. Development of an oral drug delivery system targeting immune-regulating cells in experimental inflammatory bowel disease. J. Pharmacol. Exp. Ther. 292, 15–21.

Nakaoka, R., Tabata, Y., Ikada, Y., 1995. Enhanced antibody production through sustained antigen release from biodegradable granules. J. Control. Release 37, 215–224.

Orapin, P.R., Richard, K., James, S., 1993. Albumin microspheres as a drug delivery system: relation among turbidity ratio, degree of cross-linking, and drug release. Pharm. Res. 10, 1059–1065.

Roco, M.C., 2008. Possibilities for global governance of converging technologies. J. Nanopart. Res. 10, 11–29.

Song, L.X., Bai, L., Xu, X.M., He, J., Pan, S.Z., 2009. Inclusion complexation, encapsulation interaction and inclusion number in cyclodextrin chemistry. Coord. Chem. Rev. 253, 1276–1284.

Taher, N., Alona, R., Abraham, N., Simon, B., 2009. Novel double coated nanocapsules for intestinal delivery and enhanced oral bioavailability of tacrolimus, a P-gp substrate drug. J. Control. Release 133, 77–84.

Venkataramanan, R., Swaminathan, A., Prasad, T., Jain, A., Zuckerman, S., Warty, V., McMichael, J., Lever, J., Burckart, G., Starzl, T., 1995. Clinical pharmaco-kinetics of tacrolimus. Clin. Pharmacokinet. 29, 404–430.

Vogel, V., Langer, K., Balthasar, S., 2002. Characterization of serum albumin nanoparticles by sedimentation velocity analysis and electron microscopy. Prog. Colloid Polym. Sci. 119, 28–33.

Weber, C., Coester, C., Kreuter, J., 2000. Desolvafion process and surface characteristics of protein nanoparticles. Int. J. Pharm. 196, 197–200.

Yun, M., Micheal, E.B., Dolores, T., Harriet, D., Uday, B.K., 2007. Human serum albumin nanoparticles for efficient delivery of Cu, Zn superoxide dismutase gene. Mol. Vis. 13, 746–757.